5-2010

Activity-Dependent Sharpening of the Retinotectal Map in Zebrafish: The Role of the Par Complex

Laura Mariconda
University at Albany, State University of New York

Activity-Dependent Sharpening of the Retinotectal Map in Zebrafish:

The Role of the Par Complex

Laura Mariconda

Biology Honors Program

Spring 2010

Mentor: Dr. John T. Schmidt

Abstract

Visual activity acts via NMDA (*N*-methyl *D*-aspartate) receptors in order to refine developing retinotectal maps by shaping retinal arbors. In zebrafish larvae, each arbor forms synapses by adding and deleting many trial and error branches. Branches with synapses in retinotopic sites are selectively stabilized and new branches are added next to existing synapses, while distant branches are deleted. The resulting arbor is compact and has a bushy appearance. When NMDARs are blocked, arbors become larger and dynamic rates increase almost twofold, suggesting that the release of a stabilizing signal has been prevented. A likely suspect for this retrograde stabilizing signal is arachidonic acid (AA), and this is for a few reasons. Firstly, Ca^{++} entering through NMDARs activates phospholipase A2 (PLA2) to release AA, and blocking PLA2 has the same effect as blocking NMDARs. Lastly, exogenous AA reverses the dynamic effects of NMDA blockers, such as MK801. Furthermore AA, released by DAG lipase, activates Protein Kinase C (PKC) which in turn phosphorylates GAP43 in order to stabilize F-actin.

The polarity complex, consisting of Par3, Par6, and aPKC, has been found to play a central role in neuronal polarity. It is selectively localized to the growth cones of axons, and is required for specification of the axon (Banker 2008). Moreover, the polarity complex's role in cell polarization is significant since it promotes the growth of actin filaments and microtubules, as enhanced axon outgrowth requires drastic rearrangements of actin filaments and microtubules within axonal growth cones (Yoshimura et al., 2006). As aforementioned, retinal axons have many trial and error branches, and it is hypothesized that each branch may reassemble the polarity complex before it grows out. A system for antisense suppression of either Par3 or Par6 in retinal ganglion cells was developed in order to test its effects on retinotectal arbors. After labeling zebrafish retinal ganglion axons with DiO on Day 2, images were taken the next day of

the newly fluorescent arbors and analyzed as before treatment images. Then, the eyes of zebrafish larvae were injected with antisense oligonucleotides suppressing either Par3 or Par6 (100uM every 8 hours), and then reimaged after 24 hours. In some cases, the treatment was continued for another day and the arbor was imaged after two days of treatment.

Overall, the width, and area of the treated arbors did not differ from the controls before or after treatment. However, the length of the Par6 arbors did show a slight increase in length. Additionally, treated arbors experienced less branching than the controls. On Day 3 (before treatment), the experimental and control arbors had similar numbers of branches (12.73 +/-1.11 vs. 11.83 branches +/-0.70, respectively). By Day 4, however, the control arbors had a mean value of 15.05 +/-1.36 branches, whereas arbors treated with Par3 antisense and Par6 antisense had mean values of 13.55 +/-1.63 and 10.06 +/-1.07 branches, respectively. These numbers indicate that arbors treated with the antisense oligos added fewer branches than the controls, and in some cases, added none at all.

Suppression of Par3 and Par6 indeed had a differential impact on immature and mature arbors. Small arbors experienced less branching than the controls, but arbors beginning with more branches tended to maintain them and even added new ones. In contrast, the overall growth of the arbors was unaffected, indicating that the antisense suppression targets branch formation, and not the size of the arbors. Furthermore, these changes in growth patterns indicate the polarity complex might need to be activated and reassembled for branch formation as predicted.

Table of Contents

Introduction

During development, the retina grows axons through the optic nerve into the brain to form a retinotectal map. The initial crude map is set up by gradients in the retina and tectum (Cheng et al, 1995), but normal patterned visual activity and synaptic transmission guide the remodeling of axonal processes in the development of the retinotectal map (Ruthazer et al, 2006). This is accomplished via the activity of NMDA receptors which regulate the addition, deletion, and stabilization of branches as arbors grow. Retinal axons add and delete many trial and error branches (Harris et al, 1987), and NMDA receptor activation selectively stabilizes branches with synapses in retinotopic sites and triggers new branch formation nearby (Meyer et al, 2006), while distant branches are deleted. The NMDA receptor detects correlated activity, and thus is able to identify synchronous activity from neighboring ganglion cells of the same receptive field type. These inputs are then stabilized and retinotectal maps are modified and finalized (Schmidt et al, 1995). Overall, this results in a sharpened retinotectal map.

The refinement of the retinotectal map is reflected in the dynamic branching of arbor which is guided by visual stimulation and NMDAR activity as previously indicated. Ruthazer et al. (2006) found that synaptogenesis and synaptic maturation play a significant role in the structural development of axonal projections, as attested by the aforementioned stabilization of branches as a result of NMDAR activity. This was accomplished by labeling sites of synapse formation, thereby revealing the distribution and dynamics of presynaptic sites within retinotectal axons. It was found that axon arbor dynamics are specifically affected by synaptic contacts (Ruthazer et al, 2006). Axon branches retract past faintly labeled synapses but are locally stabilized at intensely labeled synapses. Additionally, new branches form almost exclusively at newly formed synapses (Meyer et al. 2006). Stabilized nascent branches invariably

bear synapses, and the dynamics of branch retraction suggest strongly that nascent synapses can act at branch tips to prevent retraction. These observations thus provide evidence that synaptogenesis guides axon growth firstly by promoting initial branch extension and secondly by selective branch stabilization (Meyer et al, 2006).

Taken as a whole, these findings suggest the development of axonal arbors consists of the extension of exploratory side branches that make many immature synaptic contacts with postsynaptic target neurons. The majority of these contacts are lost over time, but a few succeed in maturing and stabilize (Ruthazer et al, 2006). In turn these new stable synaptic sites become part of the stable core arbor and serve as points for additional exploration by new branches. Lastly, a noteworthy finding concerning visual stimulation indicates that it actually slows axonal growth by reducing exploratory branch extension through stabilization (Ruthazer et al, 2006). It is through these processes of visual activity and synaptogenesis that we see the mechanism by which NMDA receptors stabilize and shape developing arbors.

When NMDARs are blocked, axonal branch additions and deletions significantly increases, which suggests that the release of a stabilizing signal has been inhibited (Leu & Schmidt 2008). Arachidonic acid has been proposed to be this retrograde signal since Ca^{++} entering through NMDARs activates phospholipase A2 (PLA2) to release AA, and blocking PLA2 has the same effect as blocking NMDARs. A second reason AA is likely a retrograde signal is because exogenous AA reverses the increased dynamic rates caused by MK801 (Leu & Schmidt, 2008). Once released by cytoplasmic phospholipase 2 (cPLA2), DAG lipase releases AA upon activation of NMDA receptors postsynaptically (Lom et. al., 1997). AA in turn activates PKC to phosphorylate GAP43 which in turn leads to the stabilization of F-actin. Blocking presynaptic PKC dramatically stops branching, suggesting that other PKC substrates may be involved.

One such substrate consists of the polarity complex (Par3, Par 6 and atypical PKC) which has previously been found to play a significant role in the initiation of an axon. In order to activate the complex, PKC phophorylates Par3. This complex underlies the selection of a single axon from multiple neurites (Shi et al, 2003). Although the mechanisms by which this occurs have remained elusive, significant progress has been made toward understanding the many intracellular signaling cascades during neuronal polarization. Once such cascade includes the positive feedback loop composed of Cdc42, the Par complex, and Rac 1. Initiated by PIP3 accumulation, the Par3/Par6 complex mediates the signal from Cdc42 to Rac1 which organizes microtubules and F-actin at the axon tip, leading to axon specification (Yoshimura et al, 2005). It has been proposed that the Par-3-Par-6 complex mediates the aforementioned Cdc42-induced Rac activation by means of STEF/Tiam1. STEF/Tiam1 are Rac-specific guanine nucleotide-exchange factors, and it has been found that Par-3 directly interacts with STEF forming a complex with Par-3-aPKC-Par-6-Cdc42-GTP (Nishimura et al, 2005).

Further, the function of the Par-3–Par-6–aPKC protein complex depends on its subcellular localization in polarized cells. While it is known that Par-3 accumulates at the tip of growing axons in neurons, the particular molecular mechanism of this localization remains unknown. However, Nishimura et al. identified a direct interaction between Par-3 and KIF3A, (a plus-end-directed microtubule motor protein that delivers the complex to the axon tip), and showed that aPKC can associate with KIF3A through its interaction with Par-3. Upon disruption of Par-3–KIF3A binding, the accumulation of Par-3 and aPKC at the tip of neurites was inhibited and resulted in abolished neuronal polarity (Nishimura et al, 2004). These findings suggest that Par-3 is transported to the distal tip of the axon by KIF3A and that the proper localization of Par-3 is required to establish neuronal polarity.

In conclusion, each retinal arbor makes synapses by forming trial and error branches. At retinotopic sites, branches are stabilized and new ones are added, while distant branches are deleted. We propose that forming a new branch is similar to the making of the initial axon since both require the same cytoskeletal reorganization as well as PKC activity. Therefore, we hypothesize that each branch must reassemble the Par-3-Par-6-aPKC complex before it grows out.

While the Par complex is known to effect axon specification and maturation as previously indicated, this experiment investigated whether or not the Par complex is necessary for retinotectal branch formation. This was accomplished by suppressing either Par3 or Par6 with specific antisense oligonucleotides in zebrafish larvae. The following experiment focuses on the antisense suppression of the Par complex. Antisense oligonucleotides for Par3 and Par6 were used to suppress the effects of the Par complex, and test for effects on retinotectal arbor branching.

Methods and Materials

Collection of Eggs

Zebrafish were the subject of experimentation. They were housed in one gallon tanks containing reverse osmosis water, and were maintained in a zebrafish module (Maine Biotech, Beverly, MA) that keeps the tank water constantly flowing and fresh. Roughly 5 to 8 fish are placed in each tank according to their age as well as their ability to get along with the other fish. Salinity, pH and temperature levels of the tanks were monitored daily. Salinity was maintained around 0.5-0.8, pH around 6.4-6.7, and the temperature was between 25-27 °C. Low salinity was adjusted by adding sea salt, and the pH was adjusted upward by adding $NaHCO_3$ as necessary.

On days when collecting eggs, a series of steps were followed. First, the fish were placed in a smaller-size tank which contains a netted filter at the base, so that the fish would not be able to eat the eggs as they were laid. The next morning at light onset, the fish were placed in an incubator at about 28 ºC for roughly 90 minutes. After the eggs were laid, the fish were put back in their home tanks, and the remaining water containing the eggs was poured through a net. The eggs trapped in the net were then put in a dish, about halfway filled with tank water, and were counted and then recorded. Lastly, the eggs were transferred to a dish containing embryo medium to ensure their health and survival. For every 100ml of medium, 95.9ml of distilled water was mixed with 2-3ml of phenylthiocarbamide (concentration of 1 mg/ml) suppress pigment cells, and 16 ul t-butyl-a-phenyl-nitrone (concentration of 1.77 mg/10ml) to prevent fading of florescence. Further, the embryo medium was kept at a pH of 7.2 using NaOH (Westerfield, 1994). Lastly, the beakers were placed into a low-light incubator and maintained at a temperature around 28. ºC.

DiO Injections

Late on Day 2, DiO labeling was performed on the embryos in order to label retinal ganglion cells and their axons growing in the tectum. If the embryos hadn't hatched from their shells, two fine tipped probes were used to aid in pulling apart the shell to release the larvae, a process otherwise known as artificial hatching. The embryos were anaesthetized with a few drops of the anesthetic tricaine methane sulfonate (0.007 % TMS) and then, using a micropipette, were placed on an agar-filled Petri dish containing 6 troughs. Next, using a blunt tipped probe, the larvae were positioned so that the ventronasal quadrant of the right eye was exposed for viewing under a dissecting microscope. Excess water was removed from within the troughs so that the fish adhered to the agar. Following this, DiO labeling was performed. A 0.01% DiO solution in ethanol was placed in a micropipette with a tip diameter of 1-2µm and utilized for pressure-injection into the right eye of the larvae using a Picospritzer II with a pulse duration of 5 to 25 ms x 45psi. The DiO was successfully injected when an area of green formed at the injection site. Following the injection of the DiO, the larvae were kept under dim red light in wells filled with embryo medium and placed back in the incubator.

Imaging of Arbors

Early on Day 3, about 72 hours post fertilization (hpf), the injected embryos were embedded in agar on slides for imaging. The slides were outlined with a gel square which contained a layer of agar about 1mm high. Two troughs were sliced in the agar using a scalpel, and two anaesthetized larvae were placed into each trough using a fire polished pipette. The larvae were arranged in the troughs using a blunt tipped probe, and then the water was removed with a Kimwipe. After this, low melting point agar was added to each trough with a pipette in order to create a suitable surface for imaging and to secure the larvae in the proper orientation. Before the agar hardened, the fish were positioned dorsal side up using a fine tipped probe,

keeping their heads and chins slightly raised. Once embedded properly, they were examined on an Olympus BH2 microscope equipped for epifluorescence microscopy. After the tectum was located, a DAGE IFG 300 cooled, integrating CCD camera with a 3.3x photo eyepiece coupler was used for taking the images of the fluorescent arbors where they were displayed via Metamorph Imaging System and stored on a computer. The images were taken at 2µm depth intervals to ensure the entire three-dimensional arbor was captured. Upon completion of the time-lapse imaging, the embryos were transferred to a box lined with damp Kimwipes, and sealed with a red filter at its top in order to prevent fading of the fluorescence. The container was kept in an incubator overnight between Day 3, Day 4, and Day 5.

Par 3 and Par 6 Antisense Injections & Later Imaging

Later on Day 3, antisense oligonucleotides (21 nucleotides with phosphorothioate end linkages, complementary to the first 7 codons of zebrafish Par3 and Par6) were injected into the embryos' eyes at concentrations of 100µm. Specifically, the phosphorothioate linkage at each end of the oligonucleotide is made to resist enzymatic degradation by DNAses. The 21 nucleotide sequences of both the Par6 oligo (5'-TTT ATT AAA ACT CCG GTT CAT-3') and Par3 oligo (5'-CCC AAA ACA CAC CGT CAC TTT- 3') were used to bind the Par6 mRNA and Par3 mRNA, respectively, starting at the initiation codon. These regions were targeted in order to prevent the ribosomes from beginning translation. Injections were repeated every 8 hours to maintain suppression. After 24 hours, the arbors were reimaged at ½ hour intervals, and compared to the control growth progression from Day 3 to Day 4. The injections were continued on the same schedule, and if the fluorescence remained visible in the tectum on Day 5, further images of the arbors were taken and analyzed.

Analysis of Arbors

Metamorph Imaging System is the computer program that was used for the capturing and analysis of all the images. Since the images were taken in 2μm depth increments, they needed to be reconstructed by cutting and pasting them into a single, flattened image of the arbor. This process was followed for each day's image, and after completion, the lengths of the terminal branches (TB) as well as the inter-branch segments (IBS) were measured by using a specialized drawing tool in the Metamorph system. The length of each TB was found by measuring the distance from the tip of the branch back to where it originally branched out from the arbor. Each IBS was found by measuring the distance between two branch points. Next, a convex polygon was drawn around all of the branch tips in order to measure the area (Figures 1A and 1B). The arbor length was measured by drawing a line from the first branch point to the farthest branch tip. Furthermore, the width was found by drawing a line perpendicular to the length at the arbor's widest point. All of these values were entered in an Excel Spreadsheet for further analysis.

After reconstruction and measurement of each arbor, the images were arranged in a montage and printed out. Each arbor was traced over with a pen to more clearly show its branches. The order of each TB was determined by counting the number of branch points beginning from the parent axon and ending at the tip. After this, the sum of the orders was divided by the total number of terminal branches, resulting in the average order (AO). Finally, the maturity index (MI) was calculated by dividing the total number of branches by the highest order (HO) in the arbor. This information was also recorded in Microsoft Excel.

A dynamic analysis was accomplished by recording the additions, deletions, and growth of the branches during the time lapse imaging. This was made possible by labeling each branch with a unique identifier that would allow for its identification in successive images. Branches

that appeared in later images were given a new identifier, and branches that disappeared were considered to be deleted. This data was then compared with the data from the control arbors.

Once all of the data was compiled, bar graphs were generated via the computer program GraphPad Prism 2.01 in order to visualize the results and observe any noticeable trends or significance. This was ultimately made possible by performing Student t-tests on the arbors. Significance was measured according to how an arbor's length, width, area, number of branches, average order, sum of branch lengths, average branch length, average inter-branch length, highest order and maturity index compared to that of the controls. Significant differences were recorded in the aforementioned Excel Spreadsheet and were represented by the specific symbols located above the necessary bars in each graph.

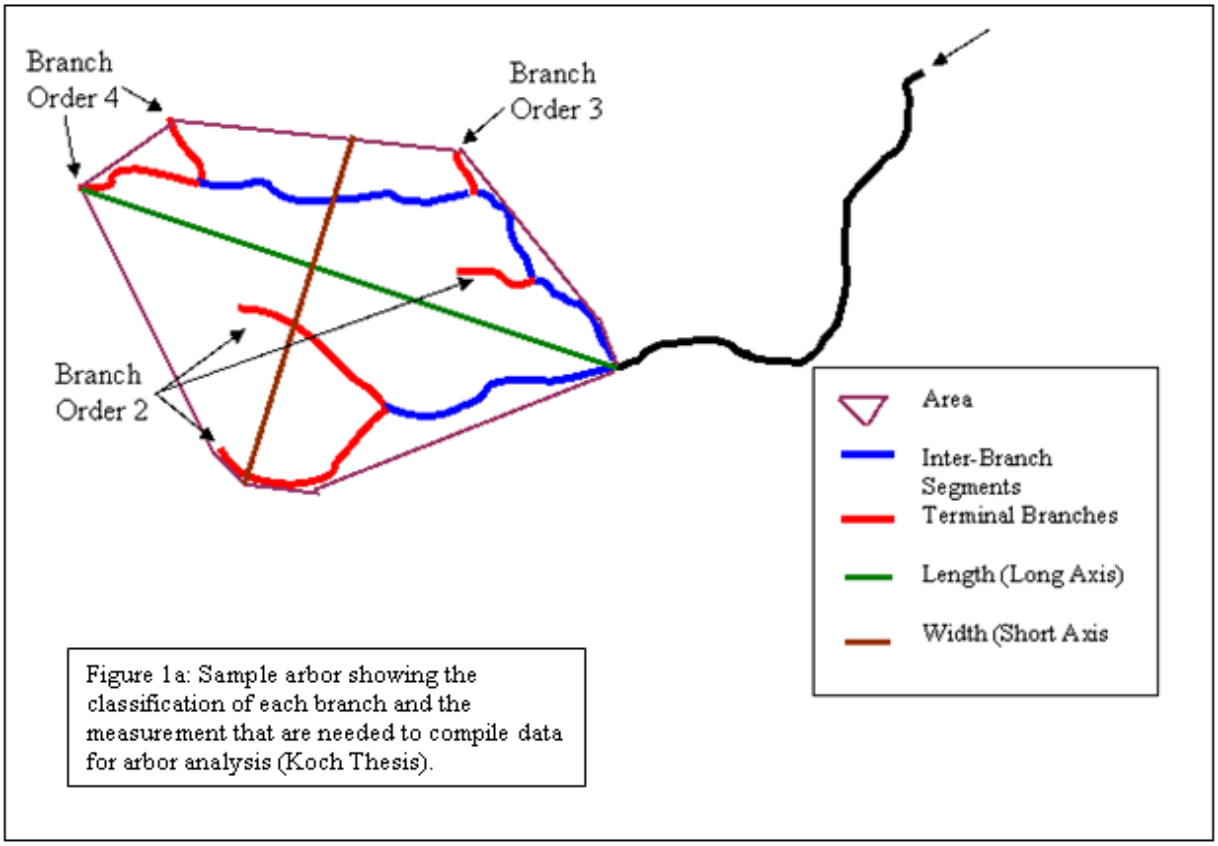

Figure 1a: Sample arbor showing the classification of each branch and the measurement that are needed to compile data for arbor analysis (Koch Thesis).

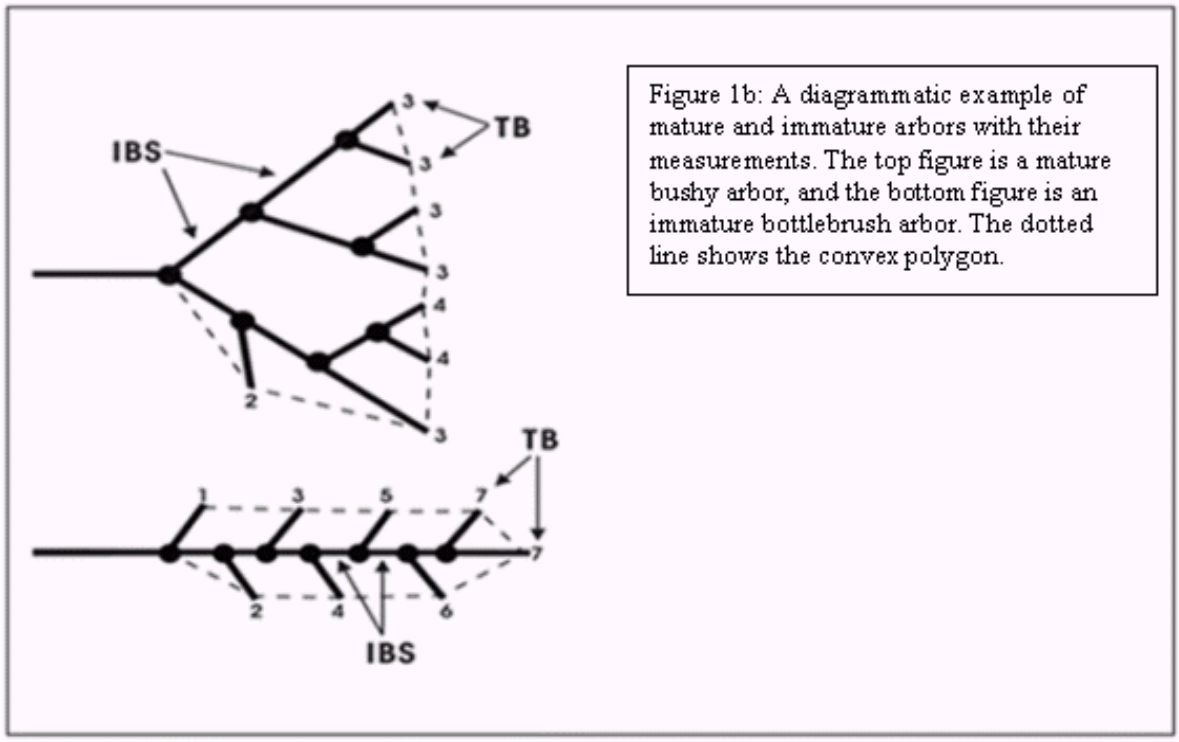

Figure 1b: A diagrammatic example of mature and immature arbors with their measurements. The top figure is a mature bushy arbor, and the bottom figure is an immature bottlebrush arbor. The dotted line shows the convex polygon.

Results

Control Arbors

Two groups of control arbors were created for this experiment. Experimentation for the first group was conducted via a longitudinal design, in which the same 34 arbors were treated and imaged from Day 3 to Day 4 as for the experimental arbors. Figure 2 is an illustration of a group of four such arbors. Similar to the experimental group, this group of arbors underwent injections; however they were injected with scrambled oligos and Ringers, rather than oligos alone specific for either Par3/Par6 suppression. This was done to ensure that the mere act of injecting did not have any effects on the development of the arbor.

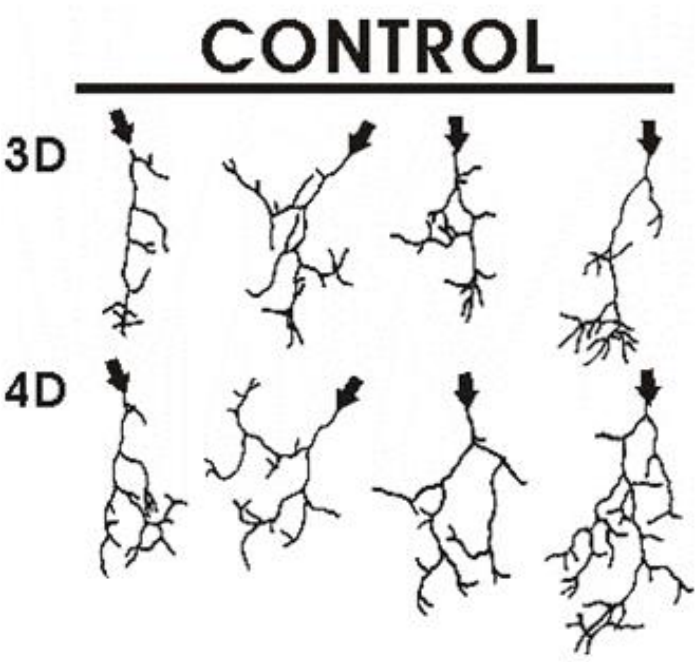

FIGURE 2: A set of four control arbors showing growth differences between Day 3 (3D) and Day 4 (4D).

The second group of control arbors was analyzed via a cross-sectional study, in which a set of arbors was imaged on a Day 3, a different set on Day 4, and another set on Day 5. No same

set of arbors were imaged serially from Days 3 to Day 5. Further, this control group did not receive injections of any type. However, since cross-sectional studies are not as powerful as longitudinal ones, data from both groups were combined to ensure the results were accurate.

A second alteration had to be made while analyzing the control arbors. On average, the experimental arbors commonly had fewer branches on Day 3 than the controls, which could reduce the accuracy of the results if not teased out. This was solved by only using control arbors with 16 or fewer branches on Day 3 for comparisons. This way both control and experimental arbors were similar on Day 3, and the results would be unbiased. To ensure the control arbors with 16 or fewer branches yielded the same results as the larger group of longitudinal controls with more than 16 branches, a t-test was performed on the two groups (Table 1). This data shows that indeed no significant differences were found between the two groups on Day 3.

Table 1: T-test for Controls #Br<16 vs Uninjected

n=35	L	W	A	# Br	Avg. Or	Sum BL	Avg. BL	Avg. IBL	Hi Or	M.I.
D3CTL <16	29.94	15.59	343.75	11.83	4.98	85.83	3.86	5.04	7.83	1.51
SEM	2.01	1.10	41.95	0.70	0.24	5.37	0.23	0.73	0.44	0.05
t-test	0.39	0.12	0.21	0.37	0.48	0.36	0.30	0.15	0.25	0.41

Once all of the aspects of the control groups were standardized, aspects of size and branching were measured in order to make comparisons between the complexity of the controls and the treated arbors. Tables 2 and 3 show control arbor branching data and size data, respectively, from the first group. Similarly, Tables 4 and 5 show arbor branching and size, respectively, from the second group.

Table 2: Injected Control Arbor Branching- Longitudinal Set					
Arbor Branching Day 3 N=35			Arbor Branching Day 4 N=35		
Measure	Average	SEM	Measure	Average	SEM
No. Branches	14.97	0.84	No. Branches	15.37	1.09
Avg. Order	5.72	0.23	Avg. Order	5.15	0.26
Avg Br Length (µm)	3.81	0.15	Avg Br Length (µm)	4.22	0.22
Inter Br Length (µm)	4.39	0.48	Inter Br Length (µm)	5.31	0.35
Table 3: Injected Control Arbor Size- Longitudinal Set					
Arbor Size Day 3			Arbor Size Day 4		
Measure	Average	SEM	Measure	Average	SEM
Length (µm)	29.94	2.01	Length (µm)	34.08	2.68
Width (µm)	15.59	1.1	Width (µm)	19.76	1.38
Area (µm2)	343.75	42.0	Area (µm2)	522.2	71.06
sumBL (µm)	85.83	5.37	sumBL (µm)	122.1	10.84

Table 4: Control Arbor Branching- All Arbors								
Arbor Branching Day 3 N=118			Arbor Branching Day 4 N=93			Arbor Branching Day 5 N=34		
Measure	Average	SEM	Measure	Average	SEM	Average	Control	SEM
No. Branches	15.19	0.49	No. Branches	16.84	0.69	No. Branches	17.27	1.14
Avg. Order	5.72	0.13	Avg. Order	5.69	0.18	Avg. Order	5.61	0.28
Avg Br Length (µm)	3.74	0.08	Avg Br Length (µm)	4.59	0.20	Avg Br Length (µm)	5.01	0.30
Inter Br Length (µm)	4.34	0.31	Inter Br Length (µm)	5.87	0.52	Inter Br Length (µm)	6.36	0.59
Table 5: Injected Control Arbor Size- All Arbors								
Arbor Size Day 3 N=118			Arbor Size Day 4 N=93			Arbor Size Day 5 N=34		
Measure	Average	SEM	Measure	Average	SEM	Average	Control	SEM
Length (µm)	31.16	0.94	Length (µm)	36.78	1.05	Length (µm)	42.23	2.03
Width (µm)	16.87	0.28	Width (µm)	24.06	0.93	Width (µm)	26.45	1.51
Area (µm2)	408.91	24.00	Area (µm2)	671.99	38.95	Area (µm2)	838.92	75.73
sumBL (µm)	104.53	4.08	sumBL (µm)	144.68	5.78	sumBL (µm)	169.9	10.85

The data show that an increase in the control arbors in area, length, and width that correspond with increases in the number of branches, branch length, as well as inter-branch length. Ultimately, control arbors grow more branches which mainly accounts for the increase in the overall size of the arbor as there is also a slight increase in the average branch length and inter-branch length.

Furthermore, the complexity of an arbor can be determined by calculating its maturity

index (MI), which is the total number of branches divided by the highest order of branching. From this, one could conclude that an increase in the number of branches and a decrease in the highest order or average order would result in a more mature, bushy arbor and a higher maturity index. The data in Tables 2 and 4 shows that in both groups, the number of branches increased and overall the average order decreased. Therefore, control arbors become mature and bushy from Days 3 to 5.

Effects of Par3 and Par6 Antisense Suppression

Figures 3 and 4 are arbors representing growth patterns after 24 hours of antisense suppression for Par3 and Par6, respectively. They consist of actual images of the arbors, each coupled with a drawing of the arbor created by tracing over the image with a pen. Thirty-one arbors were analyzed on Days 3 through 5 after Par3 antisense suppression, and twenty four arbors were analyzed on Days 3 through 5 after Par6 antisense suppression.

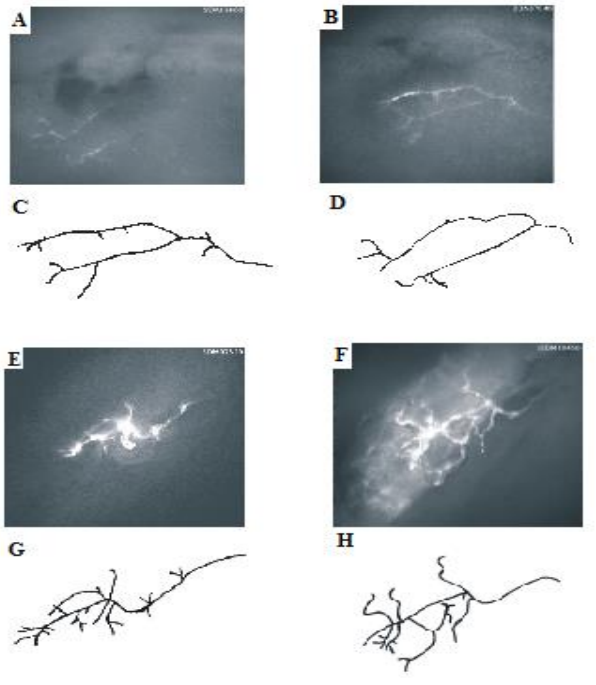

FIGURE 3: Two arbors (A and E) imaged on Day 3 and reimaged on Day 4 (B and F) after 24 hours of treatment of retina with Par3 antisense oligos. C, D, G, and H are drawings of the arbor imaged above it.

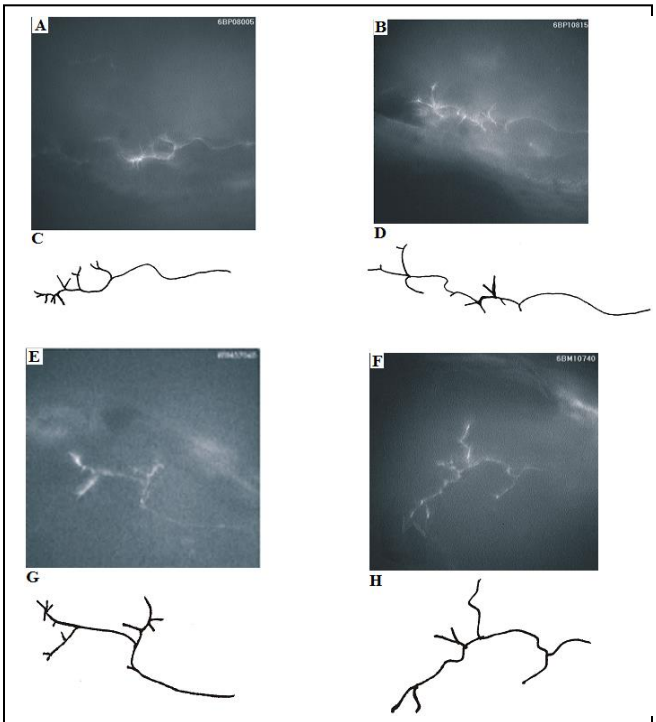

FIGURE 4: Two arbors (A and E) imaged on Day 3 and reimaged on Day 4 (B and F) after 24 hours of treatment of retina with Par6 antisense oligos. C, D, G, and H are drawings of the arbor imaged above it.

Figures 5 and 6 show samples of additional arbors representing the growth patterns as a result of Par3 and Par6 antisense suppression.

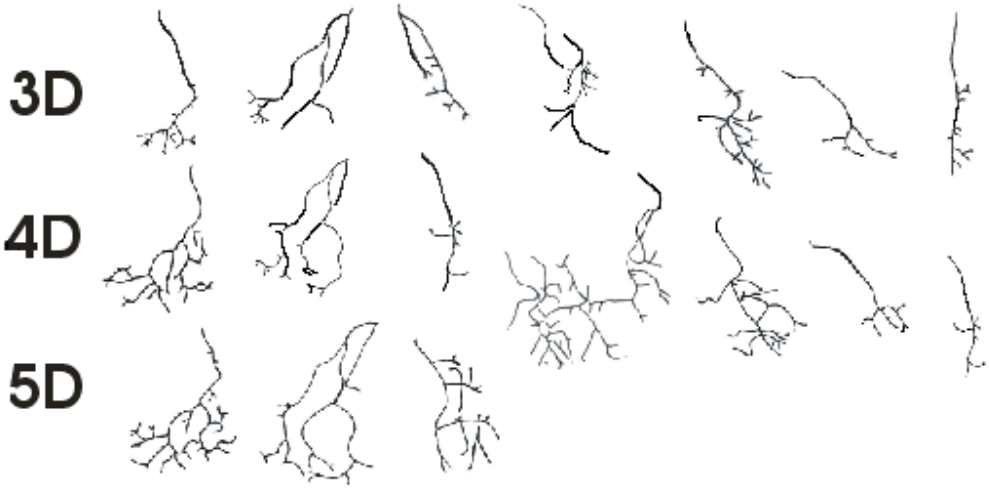

FIGURE 5: Seven arbors imaged on Day 3 and reimaged on Day 4 after 24 hours of treatment or also Day 5 after 48 hours of treatment of retina with Par3 antisense oligos.

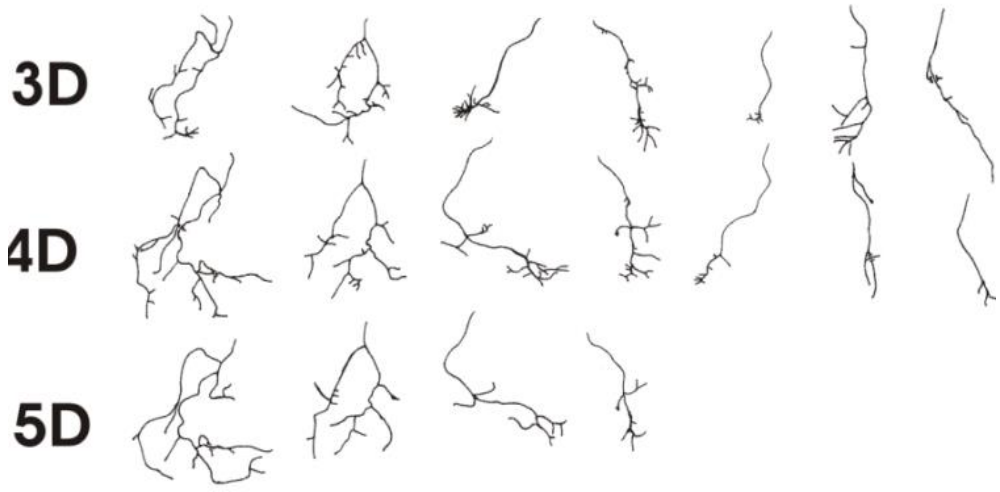

FIGURE 6: Seven arbors imaged on Day 3 and reimaged on Day 4 after 24 hours of treatment or also Day 5 after 48 hours of treatment of retina with Par6 antisense oligos.

In analyzing the above figures, it is clear that many arbors treated with either Par 3 or Par 6 antisense oligos developed similarly in size compared to controls; however, it is apparent that the treated arbors often experienced less branching.

Additionally, because arbors commonly varied in terms of complexity and branching at the onset of treatment, they tended to yield different results. Figure 7 shows the effect of Par 3 antisense suppression on two different types of arbors. Arbors with many branches (A) were less strongly affected than those with few branches (B) at the onset of treatment. Arbors starting with more branches tend to maintain them and even add a few new ones, while arbors starting with fewer branches often add no new branches at all. Arbors suppressed with Par6 showed similar effects.

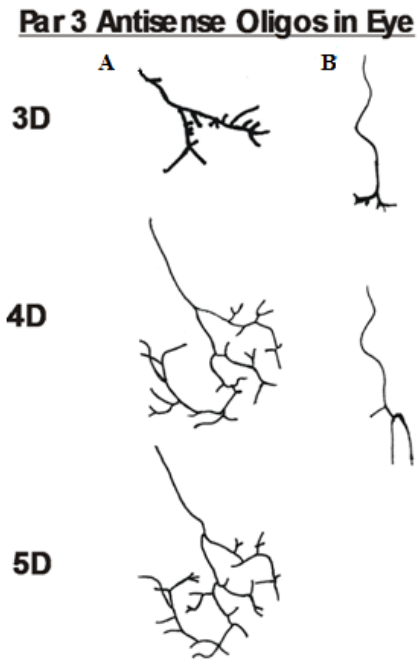

FIGURE 7: A comparison of two arbors before and after Par3 antisense suppression.

Quantitative Analysis of Arbor Branching

A more quantitative approach can be taken to analyze the growth of branches before injections and after one day of treatment (Day 4) and then after two days of treatment (day 5). Figures 8 through 10 show graphs of arbor size from Day 3 to Day 5. Figures 11 through 13 show bar graphs of arbor branching on Days 3, 4 and 5.

Before treatment on Day 3, the Par3 and Par6 arbor had no significant differences in the lengths, widths, areas and sum of branch lengths compared control injected arbors (Figure 8).

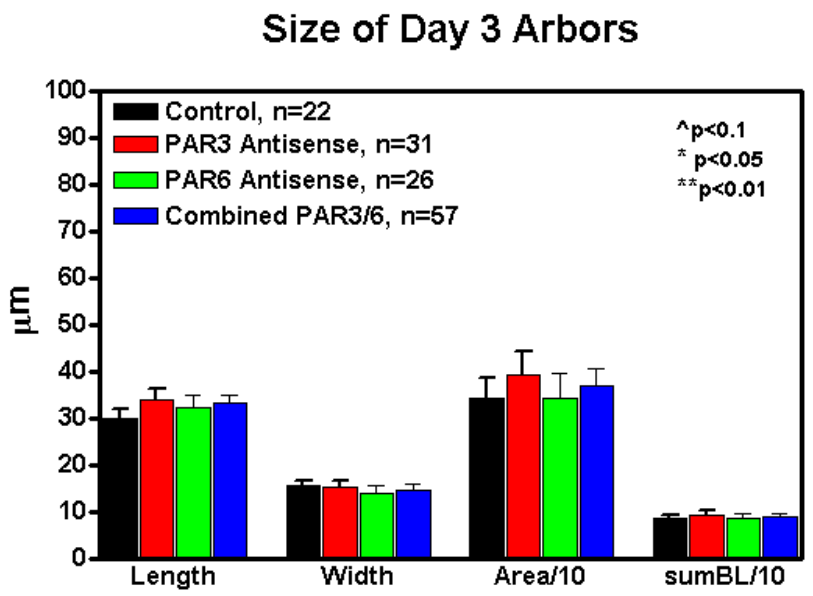

FIGURE 8: A bar graph showing the effect on size of arbors with Par3 and Par6 antisense suppression on Day 3. Table 6 is the data table for this graph.

Table 6: Size Day 3 n=57	Average	SEM	Average	SEM	Average	SEM	Average	SEM
Measure	Control	Control	PAR3 Antisense	PAR3 Antisense	PAR6 Antisense	PAR6 Antisense	Combined PAR3/6	Combined PAR3/6
Length	29.94	2.01	34.03	2.28	32.06	2.74	33.13	1.75
Width	15.59	1.10	15.29	1.29	14.04	1.67	14.72	1.03
Area/10	34.38	4.20	39.26	5.05	34.25	5.17	36.98	3.60
sumBL/10	8.58	0.54	9.33	0.79	8.53	0.96	8.96	0.61

On Day 4 and Day 5, the length, width, area, and sum of branch lengths all increased from Day 3. Small differences between the size of control arbors and Par3 and Par6 arbors were revealed after analysis (Figures 9 and 10). On Day 4, Par3 arbors as well as combined Par3/Par6 arbors showed a trend towards an increased length of the arbor (both $p<0.10$).

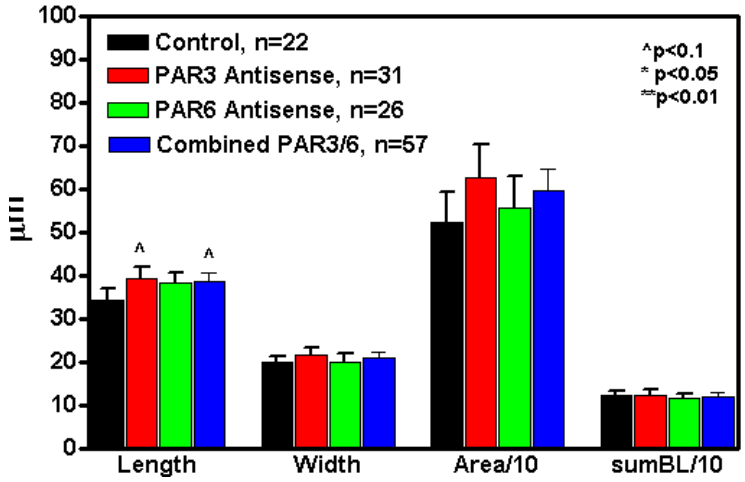

FIGURE 9: A bar graph showing the effect on size of arbors with Par3 and Par6 antisense suppression on Day 4. Table 7 is the data table for this graph.

Table 7: Size Day 4 n=57	Average	SEM	Average	SEM	Average	SEM	Average	SEM
Measure	Control	Control	PAR3 Antisense	PAR3 Antisense	PAR6 Antisense	PAR6 Antisense	Combined PAR3/6	Combined PAR3/6
Length	34.08	2.68	39.13	2.70	38.23	2.42	38.72	1.82
Width	19.76	1.38	21.64	1.58	19.86	2.07	20.83	1.27
Area/10	52.22	7.11	62.61	7.51	55.67	7.34	59.44	5.25
sumBL/10	12.21	1.08	12.28	1.21	11.50	1.07	11.92	0.87

Lastly, on Day 5, there was a significant increase in the overall length of Par3 arbors ($p<0.05$). However, this difference is small and is subject to change since only 11 arbors were imaged on Day 5. Thus, it is plausible to say antisense suppression affects primarily branch formation, and less so the overall size of the arbors.

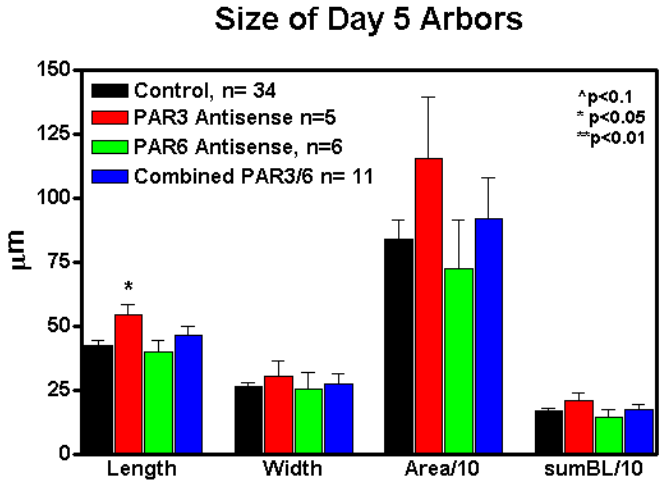

FIGURE 10: A bar graph showing the effect on size of arbors with Par3 and Par6 antisense suppression on Day 5. Table 8 is the data table for this graph.

Table 8: Size Day 5 n=11	Average	SEM	Average	SEM	Average	SEM	Average	SEM
Measure	Control	Control	PAR3 Antisense	PAR3 Antisense	PAR6 Antisense	PAR6 Antisense	Combined PAR3/6	Combined PAR3/6
Length	42.23	2.03	54.26	4.30	39.75	4.39	46.34	3.52
Width	26.45	1.51	30.14	6.24	25.34	6.54	27.52	3.96
Area/10	83.89	7.57	115.21	24.06	72.47	18.82	91.90	15.72
sumBL/10	16.99	1.09	20.67	3.08	14.17	3.16	17.13	2.35

Figure 11 shows that there were no significant differences in branching between the control and experimental arbors on Day 3, before the injections occurred. The experimental number of branches, average order, average branch length and inter-branch lengths were all rather similar to the controls. Since the branching data for both groups were so similar, we could test whether the antisense oligonucleotides produced significant changes on Day 4 and Day 5, below.

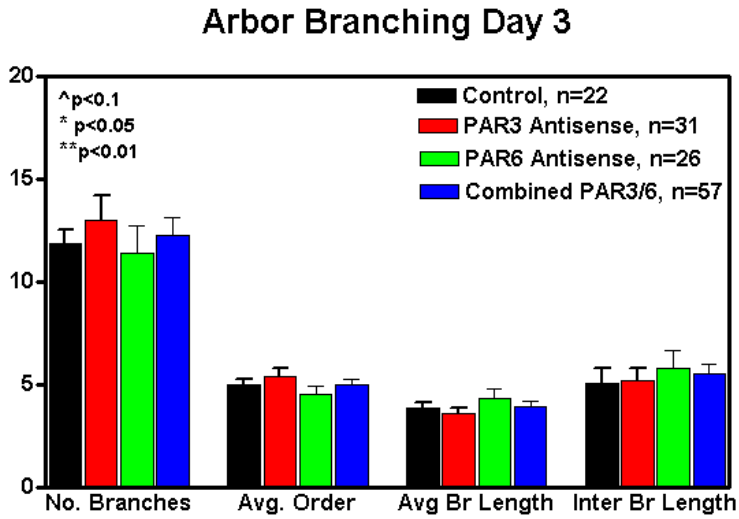

Figure 11: A bar graph representing arbor branching on Day 3, before treatment began.

Table 9: Branching Complex Day 3 n=57	Average	SEM	Average	SEM	Average	SEM	Average	SEM
Measure	Control	Control	PAR3 Antisense	PAR3 Antisense	PAR6 Antisense	PAR6 Antisense	Combined PAR3/6	Combined PAR3/6
No. Branches	11.83	0.70	13.00	1.30	11.38	1.30	12.26	0.86
Avg. Order	4.98	0.24	4.52	0.39	4.52	0.39	4.99	0.28
Avg Br Length	3.86	0.23	3.61	0.25	4.31	0.47	3.93	0.26
Inter Br Length	5.04	0.73	5.20	0.56	5.81	0.82	5.48	0.48

On Day 4, there were some significant differences between the control and the experimental arbors (Figure 12). While the number of branches in the control arbors increased, the number of branches in the Par3/Par6 arbors remained similar to the number of branches on Day 3. Further, the average number of branches following the antisense suppression of Par3 and Par6 was significantly less than the control group on Day 4. Arbors treated with Par6 antisense

had significantly fewer branches than controls ($p<0.01$), while there was a decreased trend in the number of branches in Par3 arbors ($p<0.10$). When combined, the Par3/6 arbors had significantly fewer branches than the controls ($p<0.05$). There was also a significantly lower average order for the Par3, Par6, and combined Par3/6 arbors compared to the control group ($p<0.01$, $p<0.05$, $p<0.05$ respectively). Finally, significant increases were observed in the average branch length and inter-branch length of the Par3/Par6 arbors from Day 3 to 4 (both $p<0.01$). Individually, Par6 arbors had a significant increase in average branch length and inter-branch length (both $p<0.05$), while Par3 experienced a mild increase in inter-branch length ($p<0.10$) and a more significant increase in average branch length compared to controls ($p<0.01$). These increases in average and inter-branch length are anticipated because as aforementioned, the size of the overall arbor was unaffected after antisense treatment, yet there was a decrease in the number of branches. Thus, the branch and inter-branch lengths of the arbors must have increased in order to compensate for this.

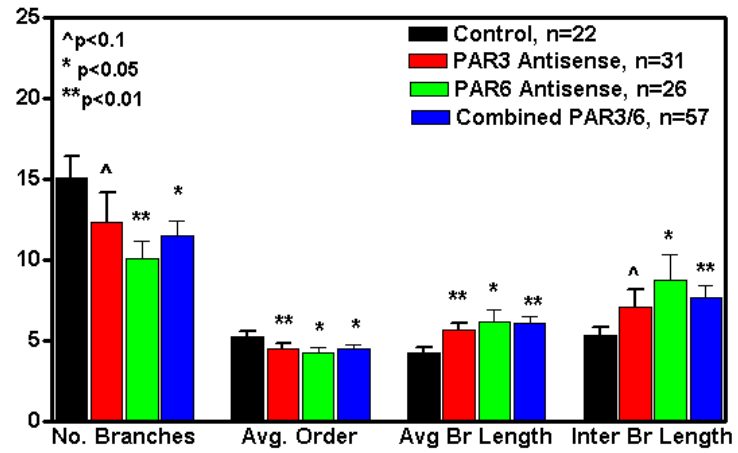

Figure 12: A bar graph representing arbor branching on Day 4 after 24 hours of treatment.

Table 10: Branching Complex Day 4 n=57	Average	SEM	Average	SEM	Average	SEM	Average	SEM
Measure	Control	Control	PAR3 Antisense	PAR3 Antisense	PAR6 Antisense	PAR6 Antisense	Combined PAR3/6	Combined PAR3/6
No. Branches	15.05	1.36	12.33	1.83	10.06	1.07	11.46	0.90
Avg. Order	5.23	0.35	4.45	0.38	4.23	0.34	4.49	0.24
Avg Br Length	4.23	0.32	5.64	0.38	6.13	0.77	6.09	0.40
Inter Br Length	5.31	0.48	7.04	1.11	8.76	1.52	7.64	0.78

Further dramatic differences can be seen in the data from Day 5 (Table 11). Figure 13 shows a slight increase in the number of branches in the control, whereas combined Par3/6

arbors had a trend toward fewer branches ($p<0.10$), with Par6 arbors showing the greatest decrease in branches ($p<0.05$) and Par3 with a smaller decrease. Also, a significant decrease in the average order was again observed in Par6 arbors ($p<0.01$) but not as signifcant in the Par3 arbors. Still, combining the Par3 and Par 6 arbors showed an overall significant decrease in average order ($p<0.05$). Finally, although the average branch length and inter-branch length of the individual Par3 and Par6 arbors did increase compared to controls on Day 5, only Par6 arbors showed an increased trend (both $p<0.10$). However, combining the two sets of arbors did show a trend in the increase of average branch lengths ($p<0.10$) and a more significant increase in inter-branch lengths ($p<0.05$). This is consistent with the effects seen on Day 4.

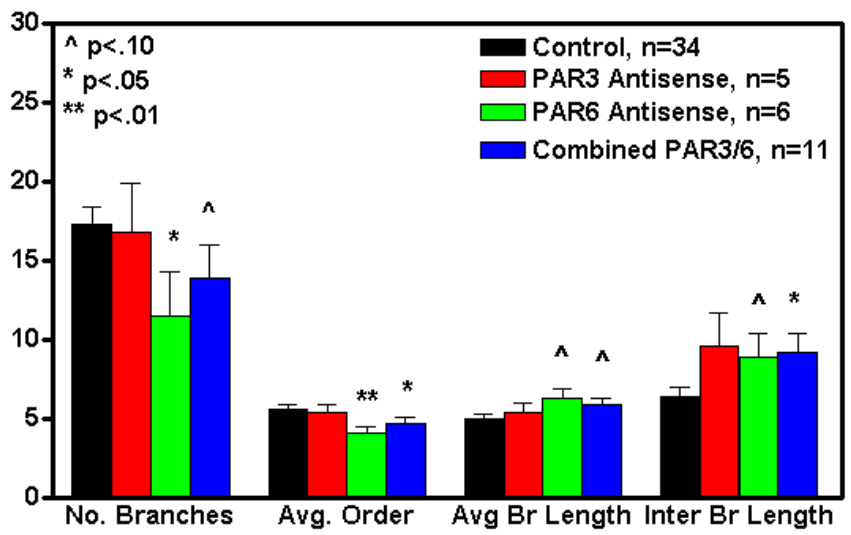

Table 11:Branching Complex Day 5 n=11	Average	SEM	Average	SEM	Average	SEM	Average	SEM
Measure	Control	Control	PAR3 Antisense	PAR3 Antisense	PAR6 Antisense	PAR6 Antisense	Combined PAR3/6	Combined PAR3/6
No. Branches	17.27	1.14	16.80	3.02	11.50	2.72	13.91	2.09
Avg. Order	5.61	0.28	5.39	0.46	4.11	0.38	4.69	0.34
Avg Br Length	5.01	0.30	5.36	0.65	6.23	0.59	5.84	0.44
Inter Br Length	6.36	0.59	9.53	2.13	8.85	1.53	9.16	1.21

Figure 13: A bar graph representing branch formation on Day 5 after 24 hours of treatment.

Lastly, Figure 14 was created to highlight the effect antisense suppression has on arbors beginning with smaller numbers of branches. It compares the number of branches added on Day 4 between both control and experimental arbors as a function of the number of branches present on Day 3. This was accomplished by subtracting the number of branches on Day 3 from the number on Day 4 and plotting this difference against the number of branches present on Day 3. Figure 14 quantitatively shows that compared to the controls, experimental arbors starting with fewer branches were more strongly affected by the treatment than those with more branches.

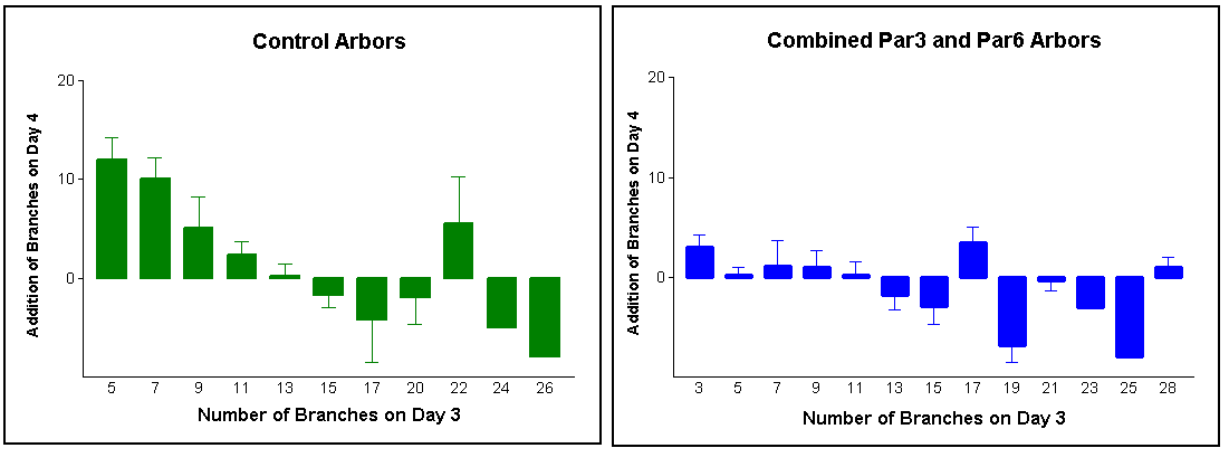

FIGURE 14: Comparison of branching between control arbors on Days 3 and 4 and arbors on Day 3 before treatment and 24 hours later on Day 4 after treatment.

In analyzing the control arbors, it is apparent that regardless of how small the number of branches a control arbor has on Day 3, it will develop into a mature arbor. On the other hand, experimental arbors with fewer branches at the onset of treatment hardly added any new ones. This is attributed to the fact these experimental arbors were not able to assemble enough Par complexes prior to treatment to fully mature.

Another way to analyze the dynamic growth of arbors is through time-lapse imagery. This was achieved by taking images of the arbors at half hour intervals. However, thus far only 6 arbors treated with antisense have been analyzed this way. According to the data collected so far on Day 4, controls added 2.30 +/- 0.35 branches/half hour interval and deleted 2.42 +/-0.35 branches/half hour interval, and Par3/Par6 arbors added 2.89 +/-.82/half hour interval and deleted 3.33 +/- 0.73 branches/ half hour interval. While these numbers suggest the experimental delete slightly more branches than controls, more data will be collected in the future to see if this trend persists.

Discussion

This experiment studied the effects of suppressing the Par3-Par6-aPKC complex in retinotectal arbors of zebrafish. Generally, the controls showed an increase in the number of branches from Day 3 to Day 4. As sharpening of the retinotopic map occurs, there are many additions and deletions of branches, though typically a greater number of branches are added. However, when the polarity complex was suppressed, there was no such increase in the number of branches from day 3 to day 4. Instead, the number of branches remained the same or even slightly decreased.

While the role of the Par complex in axon outgrowth is already known (Schwamborn et al., 2004), this effect on branching indicates that the polarity complex may need to be assembled and activated for the formation of each new branch. A look into how the Par complex contributes to axon organization, and thus the formation of new branches, can be seen in Figure 14.

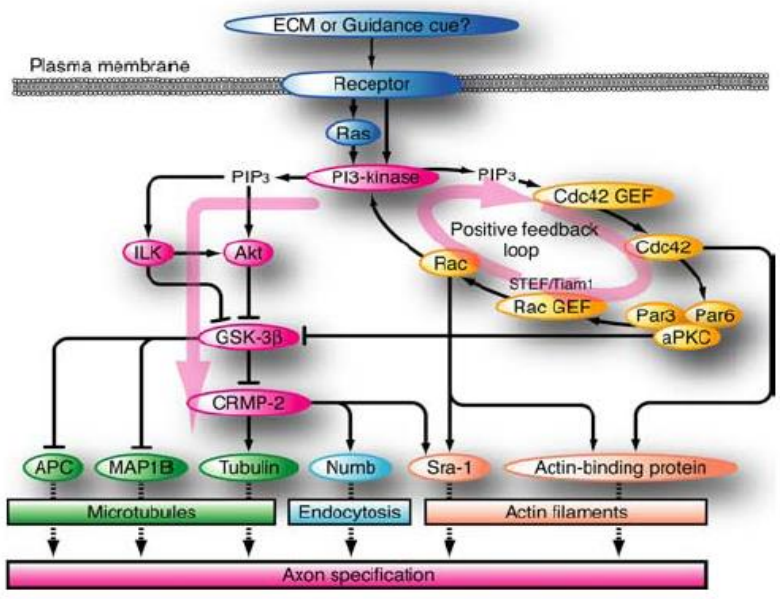

FIGURE 14: Simplified diagram of the signaling cascade involving the Par complex in axon specification (Yoshimura et al., 2006).

At the tip of an immature neurite, the extracellular matrix or growth factors activates PI3-kinase through stimulation of integrins or growth factor receptor kinases, thereby producing PI(3,4,5)P3 or PIP3. Accumulated PIP3 drives two major signaling cascades, including the positive feedback loop composed of Cdc42, the Par complex, and Rac1. Inhibiting either Par3 or Par6 leaves the neuron with no specified axon. Conversely, overexpression of the complex induces formation of multiple axons (Shi et al., 2003). We hypothesize that while the Par complex, Rac, and Cdc42 accumulate at the tip of each branch, suppression of the Par complex causes new branches to have difficulty forming but existing branches continue to grow.

This effect was heightened in immature arbors that had few branches at the onset of treatment, while arbors with many branches were less affected. This indicates that the immature arbors had not yet assembled enough Par complexes for the normal number of branches. Consequently, injecting the antisense oligos prior to most branch formation prevented new complexes from being assembled, yielding a more dramatic effect. Conversely, arbors with many branches at the onset of treatment had already activated the Par complex at each branch, and attempting to inhibit the complex at this point was essentially too late, as these arbors had developed the necessary machinery to mature and branch out.

Less dramatic effects were seen in the overall growth of the arbors. Increases in the size of the arbors were about the same as the increases in the control arbors. The length, area, and width of each arbor increased as existing branches and intermediate branches grew longer. In addition, the sum of the branch lengths was the same in spite of the decrease in the number of branches. Thus, suppression of Par3/Par6 did not limit growth overall, but specifically targeted the formation of branches.

The suppression of the Par complex had a clear effect on the growth of retinotectal arbors since overall, fewer branches were added between Day 3 and Day 4. While additions and

retractions of branches were constant, there was not a net increase in the number of branches added. Without the addition of these new branches, the arbors revealed significantly lower highest orders and average orders of branching. The treated arbors also showed significant increases in the average branch length as well as intermediate branch lengths compared to the controls. These increases came about since branches already formed on Day 3 increased in length to Day 4. This is primarily due to the fact that since new branches were unable to form, the cytoskeletal elements accumulated at the tips of existing branches focused on the extension of the branches formed on Day 3.

The effects of inhibiting the Par complex are similar to that of blocking presynaptic PKC. Previous studies have showed that blocking PKC causes near complete arrest of both growth and branching (Schmidt et al, 2004). Since PKC phosphorylation is essential for Par complex activation, it is expected that preventing its activation would have the same effects as inhibiting the expression of Par complex proteins. Further, studies indicate that AA released by DAG lipase on the presynaptic side activates PKC, and preventing its release inhibits this pathway (Schmidt et al., 2004). This produces the same effects as inhibiting the Par complex, as to be expected.

An additional way to analyze the development of arbors is through time-lapse imagery. Time-lapse imagery provides a closer look into how the arbor develops and branches out. By analyzing images that are taken within the course of 24 hours rather than from day to day, it is possible to see precisely how many branches an arbor retracts and adds as it develops. Thus far, we have minimal data on arbors analyzed imaged through time-lapse imagery. However, we will collect more time-lapse data in the future that will be sufficient for analyzing.

To understand more on the role of the polarity complex in the retinotectal arbors of zebrafish, experiments will continue to gather results on Days 3 through 5 and also to build time-lapse images to further analyze the effects on each day.

Conclusions

This experiment revealed three major findings upon suppression of the polarity complex. Firstly, the Par complex is not only required for axon elongation, but is indeed necessary for retinotectal branch formation. Secondly, arbors with the fewest branches at the onset of treatment were most affected. Lastly, suppression of Par3/Par6 did not limit growth overall, but specifically targeted the formation of branches. Future experiments involving the inhibition of other proteins involved in axonal branching could help build signaling cascades and reveal new roles of the other growth factors involved in the activity-dependent sharpening of the retinotectal map in zebrafish.

References

Alsina, B., Vu, T., and Cohen-Cory, S. 2001. Visualizing synapse formation in arborizing optic axons *in vivo*: dynamics and modulation by BDNF. *Nat. Neurosci.* 4, 1093–1101.

Banker G. 2008. "Pars, PI 3-Kinase, and the Establishment of Neuronal Polarity." Cell. 4-5.

Cheng HJ, Nakamoto M, Bergemann AD, Flanagan JG. 1995. "Complementary gradients in expression and binding of ELF-1 and Mek4 in development of the topographic retinotectal projection map." Cell 82:371–381.

Harris WA, Holt CE, Bonhoeffer F. 1987. "Retinal axons with and without their somata growing to and arborizing within the tectum of Xenopus embryos: a time-lapse video study of single fibers *in vivo*. Development 101:123-133.

Koch EJ. 2008. "Activity-Dependent Sharpening of the Retinotectal Map in Zebrafish: The Role of GAP43 and the Par Complex." Honors Thesis.

Leu BH. 2005. "Activity-Dependent Retinotectal Sharpening of Zebrafish: the Arachidonic Acid – PKC – GAP43 Pathway." PhD Thesis.

Leu BH, Schmidt JT. 2008 "Arachidonic Acid as a Retrograde Signal Controlling Growth and Dynamics of Retinotectal Arbors." Wiley Periodicals, Inc. Develop Neurobiol 68: 18-30.

Lom B, Holt CE. 1997. "Intracellular signaling cascades mediating axon extension and target recognition in the developing Xenopus visual system." Trans Am Soc Neurosci 23:350-357.

Meyer, M. P., and Smith, S. J. 2006. Evidence from *in vivo* imaging that synaptogenesis guides the growth and branching of axonal arbors by two distinct mechanisms. *J. Neurosci.* 26, 3604–3614.

Nishimura T, Kato K, Yamaguchi T, Fukata Y, Ohno S, and Kaibuchi K. 2004. "Role of the PAR-3–KIF3 complex in the establishment of neuronal polarity." 2004. Natural Cell Biology.6 (4): 328-333.

Nishimura T, Yamaguchi T, Kato K, Yoshizawa M, Nabeshima Y, Ohno S, Hoshino M, Kaibuchi K. 2005. **"**PAR-6-PAR-3 mediates Cdc42-induced Rac activation through the Rac GEFs STEF/Tiam1.**"** Natural Cell Biology. Mar;7(3):205-7.

Ruthazer ES, Li J, Cline HT. 2006. "Stabilization of Axon Branch Dynamics by Synaptic Maturation." The Journal of Neuroscience., 26(13):3594 –3603.

Schmidt JT. 2004. "Activity-Driven sharpening of the Retinoprojection: The search for retrograde synaptic signaling pathways." J. Neurobiol 59:113-114.

Schmidt JT, Fleming MR, Leu BH. 2004. “Presynaptic Protein Kinase C controls maturation and branch dynamics of developing retinal arbors: possible role in activity-driven sharpening.” J. Neurobiol 58: 328-340.

Schwamborn JC, Püschel AW. 2004. “The sequential activity of the GTPases Rap1B and Cdc42 determines neuronal polarity.” Nature Neuroscience 7 (9): 923-929.

Shi S, Jan L, Jan Y. 2003. "Hippocampal neuronal polarity specified by spatially localized mPar3/mPar6 and PI 3-Kinase activity." Cell, Vol.112, 63-75.

Westerfield, Monte. 1994. The Zebrafish Book. Eugene, OR: Univ. Oregon.

Yoshimura T, Arimura N, Kaibuchi K. 2006. “Signaling Networks in Neuronal Polarization.” The Journal of Neuroscience 26(42):10626-10630.

Yoshimura T, Arimura N, Kawano Y, Kawabata S, Wang S, Kaibuchi K. 2005."Ras regulates neuronal polarity via the PI3- kinase/Akt/GSK-3b/CRMP-2 pathway." Biochemical and Biophysical Research Communications 340:62–68